Effects of film thickness and lattice mismatch on strain states and magnetic properties of $La_{0.8}Ca_{0.2}MnO_3$ thin films

R. A. Rao,[a] D. Lavric, T. K. Nath, and C. B. Eom[b]
Department of Mechanical Engineering and Materials Science, Duke University, Durham, North Carolina 27708

L. Wu and F. Tsui
Department of Physics and Astronomy, University of North Carolina, Chapel Hill, North Carolina 27599

The effects of strain relaxation on the crystallographic domain structure and on the magnetic and transport properties of epitaxial colossal magnetoresistive $La_{0.8}Ca_{0.2}MnO_3$ (LCMO) thin films have been studied. LCMO films in the thickness range of 100–4000 Å were grown on (001) $SrTiO_3$ and (001) $LaAlO_3$ substrates, which impose an in-plane tensile and an in-plane compressive biaxial stress in the films, respectively. On (001) $SrTiO_3$ substrates, the films can be grown coherently up to a thickness ~250 Å, then strain relaxation occurs at a thickness of ~500 Å. In contrast, even the 100 Å film grown on (001) $LaAlO_3$ is partially relaxed, and the critical thickness for complete strain relaxation is ~750 Å. The very thin films (<250 Å) show a pure $(001)^T$ normal orientation for growth on $SrTiO_3$ and a pure $(110)^T$ texture for growth on $LaAlO_3$. As thickness increases, the lattice strain relaxes, resulting in mixed $(001)^T$ and $(110)^T$ textures for growth on both substrates. Both the Curie and peak resistivity temperatures increase with increasing film thickness, but they do not exhibit a correlation to strain states of the film. © *1999 American Institute of Physics.* [S0021-8979(99)35008-8]

The discovery of colossal magnetoresistance[1] (CMR) in doped manganite thin films has renewed interest in these materials for device applications.[2] One of the crucial issues in CMR manganites is the role of strain on thin film properties, including MR, and the Curie temperature (T_c). The variations of MR and magnetic properties with film thickness have been attributed[3–9] to strain states and disorder in the films. In order to study the effects of the crystal structure on magnetic and electrical transport properties of these films, it is essential to first characterize the three-dimensional (3D) strain states of the film completely, in terms of both the in-plane and out-of-plane lattice parameters. In this article we report studies of thickness and lattice mismatch dependent lattice structures and distortion in epitaxial $La_{0.8}Ca_{0.2}MnO_3$ (LCMO) films, and their influence on the magnetic properties, particularly the peak resistivity temperature (T_p) and the Curie temperature (T_c).

The LCMO films were deposited by pulsed laser ablation from a stoichiometric target on (001) $LaAlO_3$ and (001) $SrTiO_3$ substrates. While a $LaAlO_3$ substrate imposes an in-plane compressive biaxial stress on the film, a $SrTiO_3$ substrate imposes a corresponding biaxial tensile stress. The operating pressure was 400 mTorr of oxygen and the substrate temperature was held at 700 °C. The thickness of the films ranged from 100 to 4000 Å in order to study strain relaxation process. Wavelength dispersive x-ray spectroscopy confirmed that the film composition is the same as that of the target within experimental error.

The doped manganite LCMO is a distorted perovskite with a cubic lattice parameter (a_p) of 3.88 Å in the bulk. Tilting of the MnO_6 octahedra yields a tetragonal structure represented by lattice parameters $\sqrt{2}a_p$, $\sqrt{2}a_p$, and $2a_p$. All the Miller indexes used in this work are based on this tetragonal unit cell and they are indicated by a superscript ''*T*.'' Due to the tetragonal distortion, one can distinguish between the $(110)^T$ oriented [equivalent to (100) or (010) of the pseudocubic perovskite unit cell] and $(001)^T$ or *c*-axis oriented films using off-axis x-ray azimuthal (ϕ) scans, similar to epitaxial $SrRuO_3$ thin films.[10] The ability to distinguish the two orientations is essential for measuring orientation dependent magnetic and transport properties in this system.

Structural characterization of the films was carried out using a four-circle x-ray diffractometer at room temperature. The only peaks observed in the normal θ–2θ scans are from the substrate (001) and the film $\{001\}^T$ or $\{110\}^T$ reflections. No other orientations or phases were observed. Off-axis ϕ scans of nondegenerate reflections such as $(111)^T$, $(113)^T$, and $(221)^T$ were used to identify the crystal orientations and textures.[11] From the ratio of the integrated peak intensities, the amount of $(001)^T$ or *c*-axis domains in the film was obtained.

The in-plane and out-of-plane lattice parameters were determined by normal and grazing incidence diffraction (GID) θ–2θ scans. The lattice parameters and orientations were checked further by off-axis scans, including $(111)^T$, $(221)^T$, and $(113)^T$, from which the lattice parameters were calculated using least square fits. The lattice parameters obtained by this technique were found to be the same as those determined by the normal and GID scans within experimental uncertainties.

The magnetic and transport properties were measured using superconducting quantum interference divice (SQUID) magnetometry and a four-terminal method, respectively.

[a]Electronic mail: rar1@acpub.duke.edu
[b]Electronic mail: eom@acpub.duke.edu

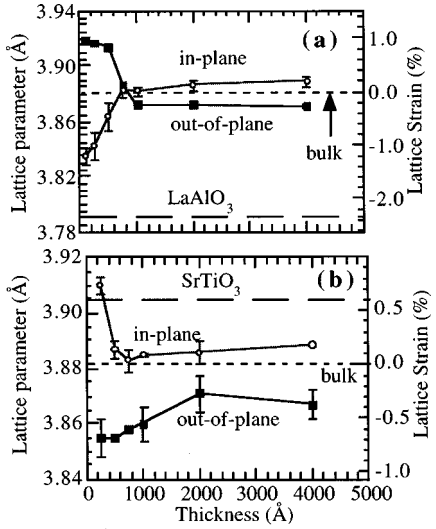

FIG. 1. Film thickness dependence of the measured out-of-plane (squares) and in-plane (circles) lattice parameters of epitaxial LCMO films grown on (a) (001) $LaAlO_3$ and (b) (001) $SrTiO_3$ substrates. The bulk parameters measured from the target and the substrate lattice parameters are indicated by the horizontal dashed lines.

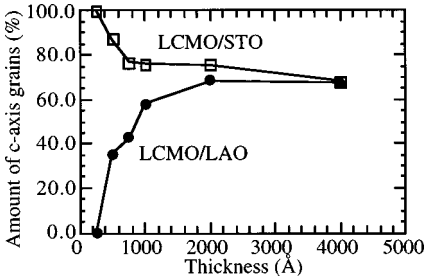

FIG. 2. Film thickness dependence of *c*-axis domains for epitaxial LCMO thin films grown on (001) $LaAlO_3$ (circles) and (001) $SrTiO_3$ (squares) substrates.

These experiments were designed to probe ferromagnetic and metal–insulator transitions. The Curie temperature T_c was determined by field-cooled magnetization measurements carried out at low fields between 1 and 10 G. The magnetization curve below the transition was extrapolated to higher temperatures and the intercept on the temperature axis was defined as T_c.

Variations of 3D strain states with respect to film thicknesses, i.e., in-plane and out-of-plane lattice parameters, for LCMO growth on the two types of substrates are shown in Fig. 1. A bulk value of 3.881 Å was obtained from the target pellet. On $SrTiO_3$ substrates, the very thin films (<250 Å), appear to be coherent in plane. In contrast, even the thinnest films grown on $LaAlO_3$ do not have the same in-plane lattice parameters as those of the substrate. In other words, these films are already partially strain relaxed. The behavior observed is believed to be caused by the different lattice mismatch between LCMO and the two types of substrates, i.e., −2.37% lattice mismatch with $LaAlO_3$ and 0.60% with $SrTiO_3$. It is expected also that a LCMO film cannot accommodate the large 2.37% compressive strain imposed by $LaAlO_3$ and it will relax even when it is very thin. This is consistent with the observation that films grown on $LaAlO_3$ continue to relax gradually from a very small thickness (<50 Å) until reaching the bulk value at ~750 Å. In contrast, the in-plane strains for the $SrTiO_3$ counterparts relax completely over a much smaller range of thickness, one between 250 and 500 Å.

The unit cell volume and bulk strain of the films were also obtained from the lattice parameter data. For very thin films, the deviation from bulk volume is quite large and, as the thickness increases, the cell volume tends to approach the bulk value. The cell volume for growth on $LaAlO_3$ increases with thickness, until reaching a maximum near 1000 Å, and then it decreases towards the bulk value. In contrast, the cell volume on $SrTiO_3$ exhibits a decrease with thickness up to 750 Å, and then it increases towards the bulk value.

While the origin(s) of the strain relaxation processes is (are) presently unknown, it is, however, clearly rooted in the initial domain structures and in how LCMO accommodates different biaxial strains in different crystal directions, particularly with respect to the MnO_6 octahedra. To explore this further, crystal domains and textures were examined. From the ratio of the integrated peak intensities between the $(001)^T$ and $(110)^T$ reflections (I_{001}/I_{110}), the number of *c*-axis domains in the film was determined, and they are shown in Fig. 2 for the two types of substrates as a function of film thickness. For the very thin films grown on $SrTiO_3$, a pure *c*-axis orientation was observed. In contrast, very thin films grown on $LaAlO_3$ show a pure $(110)^T$ out-of-plane texture with two 90 ° domains in plane. As the film thickness increases, the number of *c*-axis domains decreases for growth on the $SrTiO_3$ substrates, whereas its $LaAlO_3$ counterpart increases. This is in agreement with the transmission electron microscopy (TEM) results of Aarts *et al.*[9]

The evolution of the domain structures, shown in Fig. 2, reveals a strong connection between lattice relaxation (Fig. 1) and the resulting domain structures. For growth on $LaAlO_3$, the crossover observed between 750 and 1000 Å from in-plane compressive to tensile strain appears to coincide with the 50% *c*-axis domain crossover (see Fig. 2). For films grown on $SrTiO_3$, on the other hand, the rapid in-plane lattice relaxation observed [Fig. 1(b)] between 250 and 500 Å seems to lead to the initial appearance of $(110)^T$ textures. In the thick film limit (>2000 Å) and for growth on either substrate, the textures seem to approach an asymptotic mixture of 2/3 *c*-axis and 1/3 $(110)^T$ domains, where the strain states also reach stable values. The domain structures in this system appear to provide a pathway for lattice relaxation.

The observed crystal coherence lengths estimated from the x-ray scan widths decrease with increasing films thickness, indicated by the increase of widths with film thickness. At lower thicknesses, the full width of the rocking curve for the film is almost the same as that of the substrate, ~0.25°. Since film thickness increases are accompanied by strain relaxation, the rocking curves and ϕ scans become broader, indicating an increased mosaic spread due to multiple domain formation with strain relaxation. The full width of the rocking curve for a 4000 Å thick film is ~0.97° for growth

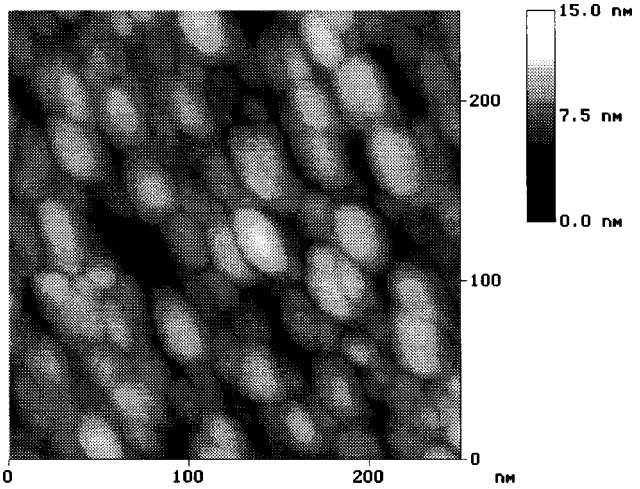

FIG. 3. STM image of a 500 Å LCMO film grown on a (001) $SrTiO_3$ substrate.

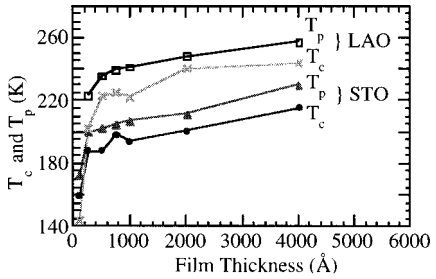

FIG. 4. Film thickness dependence of the T_p and T_c for epitaxial LCMO films grown on (001) $LaAlO_3$ (squares and crosses) and (001) $SrTiO_3$ substrates (circles and triangles).

on $LaAlO_3$, and it is ~0.78° for growth on $SrTiO_3$. The narrower rocking curves for the $SrTiO_3$ samples are consistent with the smaller lattice mismatch.

The surface morphology and the growth mechanism were also studied using scanning tunneling microscopy (STM). All the films show granular-like surface features with rounded grains, as seen in Fig. 3. As the film thickness increases, the grain size (the mean diameter of the grains) remains constant in the range of 200–500 Å. Within each grain, the root mean square (rms) roughness increases with film thickness, from 6 Å for a 250 Å film to 35 Å for a 4000 Å film. The surface roughening also appears to be related to strain relaxation. In Fig. 3 a typical STM image of a 500 Å thick LCMO film grown on (001) $LaAlO_3$ substrates is shown, where an average grain size of ~260 Å and a rms roughness of 16 Å within each grain are observed.

Finally, the effects of 3D strain states and domain structures on magnetic and transport properties were probed. The bulk pellet exhibits a metal–insulator transition with a T_p of ~260 K and a room temperature resistivity of 110 $\mu\Omega$ cm. All films studied here show suppressed T_p and T_c with respect to the bulk value. Both T_c and T_p increase with increasing film thickness, as shown in Fig. 4, while the zero temperature resistivity intercept ρ_0, decreases. The decreasing ρ_0 indicates a reduction in short range disorder. At any given thickness T_p of the film on $LaAlO_3$ is higher than its $SrTiO_3$ counterpart, which is consistent with other reports,[12,13] and it is about 10–15 K above T_c.

From the measured in-plane and out-of-plane strains, the Jahn–Teller strain (ϵ_{JT}) and bulk strain (ϵ_B), as defined in Refs. 7 and 8, have been calculated. In general ϵ_{JT}^2 decreases as the film thickness increases for both substrates, and ϵ_B exhibits different trends for the two types of substrates. However, the measured T_p and T_c of the films do not show any correlation with either ϵ_{JT}^2 or ϵ_B.

We have studied the effects of lattice strain relaxation on the crystal structure and distortion of epitaxial LCMO films with different film thicknesses and lattice mismatchs and their influence on magnetic and transport properties. As the film thickness increases, strain relaxation takes place, leading to the mosaic spread, surface roughening, and formation of mixed $(001)^T$ and $(110)^T$ domains in LCMO films that is observed. Although T_c and T_p of the films both show strong film thickness dependence, they do not show any correlation to strain states. Further investigations are necessary to elucidate the link between structural and magnetic and transport properties.

This work was supported in part by a David and Lucile Packard fellowship and by a NSF Young Investigator Award to one of the authors (C.B.E.) under Grant Nos. ONR N00014-95-1-0513 and NSF DMR-9421947, respectively. A. Second Author (F.T.) acknowledges support from the NSF under Grant Nos. DMR-9703419 and DMR-9601825.

[1] S. Jin, T. H. Tiefel, M. McCormack, R. A. Fastnacht, R. Ramesh, and L. H. Chen, Science **264**, 414 (1994).
[2] J. Z. Sun, W. J. Gallagher, P. R. Duncombe, L. Krusin-Elbaum, R. A. Altman, A. Gupta, Yu Lu, G. Q. Gong, and G. Xiao, Appl. Phys. Lett. **69**, 3266 (1996).
[3] S. Jin, T. H. Tiefel, M. McCormack, H. M. O'Bryan, L. H. Chen, R. Ramesh, and D. Schurig, Appl. Phys. Lett. **67**, 557 (1995)
[4] Y. Suzuki, H. Y. Hwang, S. W. Cheong, and R. B. van Dover, Appl. Phys. Lett. **71**, 140 (1997).
[5] J. O'Donnell, M. S. Rzchowski, J. N. Eckstein, and I. Bozovic, Appl. Phys. Lett. **72**, 1775 (1998).
[6] C. Kwon, M. C. Robson, K.-C. Kim, J. Y. Gu, S. E. Lofland, S. M. Bhagat, Z. Trajanovic, M. Rajeswari, T. Venkatesan, A. R. Kratz, R. D. Gomez, and R. Ramesh, J. Magn. Magn. Mater. **172**, 229 (1997).
[7] A. J. Millis, T. Darling, and A. Migliori, J. Appl. Phys. **83**, 1588 (1998).
[8] A. J. Millis, A. Goyal, M. Rajeswari, K. Ghosh, R. Shreekala, R. L. Greene, R. Ramesh, and T. Venkatesan (unpublished).
[9] J. Aarts, S. Freisem, R. Hendrikx, and H. W. Zandbergen, Appl. Phys. Lett. **72**, 2975 (1998).
[10] C. B. Eom, R. J. Cava, R. M. Fleming, J. M. Phillips, R. B. van Dover, J. H. Marshall, J. W. P. Hsu, J. J. Krajewski, and W. F. Peck, Jr., Science **258**, 1766 (1992).
[11] T. K. Nath, R. A. Rao, D. Lavric, and C. B. Eom (unpublished).
[12] N.-C. Yeh, R. P. Vasquez, D. A. Beam, C.-C. Fu, J. Huynh, and G. Beach, J. Phys.: Condens. Matter **9**, 3713 (1997).
[13] M. E. Hawley, C. D. Adams, P. N. Arendt, E. L. Brosha, F. H. Garzon, R. J. Houlton, M. F. Hundley, R. H. Heffner, Q. X. Jia, J. Neumeier, and X. D. Wu, J. Cryst. Growth **174**, 455 (1997).
[14] H. Y. Hwang, T. T. M. Palstra, S.-W. Cheong, and B. Batlogg, Phys. Rev. B **52**, 15046 (1995).
[15] J. M. De Teresa, M. R. Ibarra, J. Blasco, J. Garcia, C. Marquina, P. A. Algarabel, Z. Arnold, K. Kamenev, C. Ritter, and R. von Helmolt, Phys. Rev. B **54**, 1187 (1996).